THE JOURNAL OF BIOLOGICAL CHEMISTRY VOL. 288, NO. 21, pp. 15154–15166, May 24, 2013

A Lipoprotein Receptor Cluster IV Mutant Preferentially Binds Amyloid-β and Regulates Its Clearance from the Mouse Brain*

Received for publication, November 25, 2012, and in revised form, March 31, 2013 Published, JBC Papers in Press, April 11, 2013, DOI 10.1074/jbc.M112.439570

Abhay P. Sagare[‡1], Robert D. Bell[§1], Alaka Srivastava[¶1], Jesse D. Sengillo[‡], Itender Singh[§], Yoichiro Nishida[§], Nienwen Chow[¶], and Berislav V. Zlokovic[‡2]

From the [‡]Zilkha Neurogenetic Institute and Department of Physiology and Biophysics, Keck School of Medicine, University of Southern California, Los Angeles, California 90033, the [§]Center of Neurodegenerative and Vascular Brain Disorders, University of Rochester Medical Center, Rochester, New York 14642, and [¶]ZZ Alztech, Rochester, New York 14642

Background: Wild type LRP1 cluster IV (WT-LRPIV) binds plasma Aβ and reduces Aβ-related pathology in $APPsw^{+/0}$ mice.
Results: A novel LRPIV-D3674G mutant binds Aβ with a higher affinity than WT-LRPIV and clears brain Aβ better than WT-LRPIV. LRPIV-D3674G reduces effectively Aβ pathology in $APPsw^{+/0}$ mice.
Conclusion: LRPIV-D3674G is an efficient Aβ clearance agent.
Significance: Aβ clearance therapy is critical for treatment of Alzheimer disease.

Soluble low density lipoprotein receptor-related protein-1 (sLRP1) binds ~70% of amyloid β-peptide (Aβ) in human plasma. In Alzheimer disease (AD) and individuals with mild cognitive impairment converting to AD, plasma sLRP1 levels are reduced and sLRP1 is oxidized, which results in diminished Aβ peripheral binding and higher levels of free Aβ in plasma. Experimental studies have shown that free circulating Aβ re-enters the brain and that sLRP1 and/or its recombinant wild type cluster IV (WT-LRPIV) prevent Aβ from entering the brain. Treatment of Alzheimer $APPsw^{+/0}$ mice with WT-LRPIV has been shown to reduce brain Aβ pathology. In addition to Aβ, LRPIV binds multiple ligands. To enhance LRPIV binding for Aβ relative to other LRP1 ligands, we generated a library of LRPIV-derived fragments and full-length LRPIV variants with glycine replacing aspartic acid residues 3394, 3556, and 3674 in the calcium binding sites. Compared with WT-LRPIV, a lead LRPIV-D3674G mutant had 1.6- and 2.7-fold higher binding affinity for Aβ40 and Aβ42 *in vitro*, respectively, and a lower binding affinity for other LRP1 ligands (*e.g.* apolipoprotein E2, E3, and E4 (1.3–1.8-fold), tissue plasminogen activator (2.7-fold), matrix metalloproteinase-9 (4.1-fold), and Factor Xa (3.8-fold)). LRPIV-D3674G cleared mouse endogenous brain Aβ40 and Aβ42 25–27% better than WT-LRPIV. A 3-month subcutaneous treatment of $APPsw^{+/0}$ mice with LRPIV-D3674G (40 μg/kg/day) reduced Aβ40 and Aβ42 levels in the hippocampus, cortex, and cerebrospinal fluid by 60 – 80% and improved cerebral blood flow responses and hippocampal function at 9 months of age. Thus, LRPIV-D3674G is an efficient new Aβ clearance therapy.

Deposits of amyloid β-peptide (Aβ)[3] and neurofibrillary tangles are neuropathological features of Alzheimer disease (AD) (1). Aβ is produced in the brain and periphery by proteolytic cleavage from its larger Aβ precursor protein (APP) (2). A body of evidence suggests that soluble Aβ oligomer species contribute to neurodegeneration in AD (3). Aβ concentration in brain interstitial fluid is controlled by its rate of production in brain; influx and/or re-entry of circulating, peripheral Aβ into the brain across the blood-brain barrier (BBB) via receptor for advanced glycation end products (RAGE) (4); and clearance of Aβ from the brain (5, 6). Aβ is cleared from the brain by different mechanisms, including transport across the BBB via low density lipoprotein receptor-related protein-1 (LRP1) (5, 7–9) and enzymatic degradation in the brain (10). A continuous removal of Aβ from the brain and systemic circulation is essential to prevent accumulation of toxic soluble oligomeric Aβ in the brain (3, 11).

We and others have reported that cell surface LRP1 at the BBB and soluble LRP1 (sLRP1) in plasma have important functions in Aβ homeostasis (7–9, 12–21). sLRP1 is a major transport binding protein for peripheral circulating Aβ and can sequester 70 –90% of plasma Aβ in neurologically intact human

* This work was supported, in whole or in part, by National Institutes of Health Grants AG023084 and NS034467. This work was also supported by ZZ Alztech (Rochester, NY). Berislav V. Zlokovic is the scientific founder of Socratech LLC, a startup biotechnology company with a mission to develop new therapeutic approaches for stroke and Alzheimer disease. Berislav V. Zlokovic is co-inventor on patents pertaining to use of sLRP fragments as a potential therapy for Alzheimer disease.
[1] These authors contributed equally to this work.
[2] To whom correspondence should be addressed: Zilkha Neurogenetic Institute, Keck School of Medicine, University of Southern California, 1501 San Pablo St., ZNI 101, Los Angeles, CA 90089-2821. Tel.: 323-442-2566; Fax: 323-442-2145; E-mail: zlokovic@usc.edu.

[3] The abbreviations used are: Aβ, amyloid β-peptide; AD, Alzheimer disease; APP, Aβ precursor protein; RAGE, receptor for advanced glycation end products; LRP1, low density lipoprotein receptor-related protein-1; sLRP1, soluble LRP1; CR, complement-type repeat; BBB, blood-brain barrier; MCI, mild cognitive impairment; LRPIV, LRP1 cluster IV; WT-LRPIV, wild type LRP1 cluster IV; RAP, receptor-associated protein; α_2M*, activated α_2-macroglobulin; tPA, tissue plasminogen activator; MMP, matrix metalloproteinase; CSF, cerebrospinal fluid; PS, permeability surface area; aPTT, activated partial thromboplastin time; BisTris, 2-[bis(2-hydroxyethyl)-amino]-2-(hydroxymethyl)propane-1,3-diol; CBF, cerebral blood flow.

TABLE 1

Primers used in the PCR to generate constructs of the truncated fragments or mutants of LRPIV

CRs of LRPIV were cloned into pSecTag2 B vector. Full-length LRPIV (WT-LRPIV) was cloned into pcDNA3.3 TOPO vector. The forward primer has Kozak sequence (acc) and the tPA signal peptide (in italic type) followed by the LRPIV sequence.

Clone	Forward primer	Reverse primer
CR24–CR27	5′-gatcaagcttgtgacctgcgcccccaaccagttc-3′	5′-gatcggatccaaggggtgcagtctttctcg-3′
CR25–CR28	5′-gatcaagcttatgacctgtggtgtggacgag-3′	5′-gatcggatccaaagtgccgcaggcctcctcg-3′
CR25–CR27	5′-gatcaagcttatgacctgtggtgtggacgag-3′	5′-gatcggatccaaggggtgcagtctttctcg-3′
CR25–CR26	5′-gatcaagcttatgacctgtggtgtggacgag-3′	5′-gatcggatccaaaggggtgcagctctcttcatcg-3′
CR26–CR27	5′-gatcaagcttcgcacctgtgagccataccagttcc-3′	5′-gatcggatccaaggggtgcagtctttctcg-3′
CR25	5′-gatcaagcttatgacctgtggtgtggacgag-3′	5′-gagcccaaggaagagtgtgatgaattggatccgatc-3′
CR26	5′-gatcaagcttcgcacctgtgagccataccagttcc-3′	5′-gatcggatccaaaggggtgcagctctcttcatcg-3′
WT-LRPIV	5′-*accatggatgcaatgaagagagggctctgctgtgt gctgctgctGtgtggagcagtcttcgtttcgcccag ccaggaaatccatgcccgattcagaagaggagccag atccaactgcacggctagccag*-3′	5′-gcaagcttttagatgctgcagtcctcc-3′
LRPIV-D3354G	5′-ctggtggaagtgtggcaccgaggacgact-3′	5′-agtcgtcctcggtgccacacttccaccag-3′
LRPIV-D3394G	5′-ctgccttcatctgcggtggcgacaatgactg-3′	5′-cagtcattgtcgccaccgcagatgaaggcag3′
LRPIV-D3356G	5′-ccgctggcagtgcggctacgacaacgatt-3′	5′-aatcgttgtcgtagccgcactgccagcgg-3′
LRPIV-D3595G	5′-gcgctggaaatgcggtggagaccacgact-3′	5′-agtcgtggtctccaccgcatttccagcgc-3′
LRPIV-D3633G	5′-ctggcgctgtggcgcagacgccg-3′	5′-cggcgtctgcgccacagcgccag-3′
LRPIV-D3674G	5′-gcctggaagtgcggtggcgaggatgac-3′	5′-gtcatcctcgccaccgcacttccaggc-3′

subjects (14). sLRP1 levels are reduced in patients with AD and mild cognitive impairment who subsequently progress to AD (MCI-AD) (14, 22). In addition, sLRP1 is oxidized in AD and AD-MCI individuals, and oxidized sLRP1 is unable to bind Aβ (14, 22). Consequently, an increase in free, unbound Aβ plasma levels relative to sLRP1-bound plasma Aβ levels has been reported in AD and MCI-AD patients (14, 22). Experimental studies have shown that free Aβ40 and Aβ42 re-enter the brain (4, 23, 24) and contribute to the formation of neurotoxic soluble oligomeric Aβ species. It has been also reported that sLRP1 and its recombinant ligand binding domain cluster IV (LRPIV) prevent free Aβ from entering the brain (14).

Several Aβ antibody therapies are directed at facilitating Aβ clearance from the brain (25, 26). Aβ antibodies that act principally by sequestering the peripheral Aβ pool do not cross the BBB and are generally thought to clear Aβ from the brain by the so-called "peripheral sink" mechanism through binding of peripheral Aβ, which according to some studies lessens the risk of potential central side effects of the antibody clearance therapy, such as neuroinflammation, vasogenic edema, and cerebral microhemorrhages (27–30). Recent studies in patients with mild AD have shown beneficial effects of intravenous immunoglobulin preparation (Gammagard), which has been suggested to act as a peripheral sink agent containing sLRP1 and antibodies against diverse Aβ conformations (31, 32).

In a previous study, we have demonstrated that that wild type recombinant LRPIV (WT-LRPIV) effectively binds Aβ40 and Aβ42 *in vitro* (8, 14) and sequesters free Aβ in plasma of AD patients and AD transgenic mice *in vivo*, which reduces Aβ pathology in mice (14). LRPIV contains 11 complement-type repeats (CRs) (CR21–CR31), which can participate in binding of LRP1 ligands (33, 34). For example, CR24–CR28 efficiently binds LRP1 ligands Factor IXa, receptor-associated protein (RAP), and activated α_2-macroglobulin (α_2M*) (35, 36). Each CR has ~40 amino acids and a single calcium ion (35). Calcium ion binding domains are required for proper folding and structural integrity of LRP1 (33, 34). The alterations in calcium binding sites alter folding of the CRs (33). In an attempt to enhance Aβ binding to LRPIV and improve its Aβ-clearing properties, we generated a library of recombinant LRPIV fragments and full-length LRPIV variants with single glycine replacement with an aspartic acid residue in the calcium binding site in either CR 21, 22, 26, 27, 28, or 29. We expressed these LRPIV analogs in Chinese hamster ovary (CHO) cells. Next, LRP-IV-derived analogs that have been well secreted by CHO cells into the medium were purified, and their binding affinity for Aβ40 and Aβ42 and other LRP1 ligands, including apolipoprotein E2-4 (apoE2-4), tissue plasminogen activator (tPA), matrix metalloproteinase-9 (MMP-9), and Factor IXa, was determined. A lead LRPIV-D3674G mutant had the highest *in vitro* binding affinity for Aβ peptides relative to other ligands and cleared mouse endogenous Aβ more efficiently than WT-LRPIV. Moreover, subcutaneous LRPIV-D3674G treatment significantly reduced Aβ levels in brain and cerebrospinal fluid (CSF) in Alzheimer $APPsw^{+/0}$ mice and improved cerebral blood flow responses and hippocampal function. Our findings suggest that LRPIV-D3674G is an efficient new Aβ clearance therapy for AD.

EXPERIMENTAL PROCEDURES

Materials

Human Aβ40 and Aβ42 were synthesized at the W. M. Keck Facility (Yale University), using solid-phase *N-t*-butyloxycarbonyl chemistry, and purified by HPLC. Primers were synthesized by Integrated DNA Technologies (Coralville, IA), and dNTPs were obtained from Invitrogen. All other reagents were from Sigma-Aldrich unless otherwise indicated. Purified recombinant full-length wild type ligand binding cluster IV of LRP1 (WT-LRPIV) was used for generating rabbit polyclonal LRPIV antibody (GeneScript, Piscataway, NJ). Another rabbit polyclonal anti-LRPIV antibody (37) was kindly provided by Dr. Elizabeth Komives (University of California San Diego, La Jolla, CA).

Production of LRPIV Variants

Synthesis of cDNA and Cloning of LRPIV—LRP1 cDNA was synthesized from human spleen total RNA (Clontech, Mountain View, CA) using SuperScript II RT (Invitrogen). Primers were designed based on LRP1 sequence (NM_002332) (Table 1). LRPIV (Fig. 1*A*) was amplified from cDNA by polymerase chain reaction (PCR) using Pfx-DNA polymerase (Invitrogen)

and their respective primer sets and cloned into pcDNA3.3 TOPO vector. Using this construct, full-length LRPIV consisting of 11 CRs (CR21–CR31), two four-repeat fragments (CR24–CR27 and CR25–CR28), one three-repeat fragment (CR25–CR27), two two-repeat fragments (CR25-CR26 and CR26-CR27), and two single-repeat fragments (CR25 and CR26) (Fig. 1*A*) were amplified using PCR and cloned in mammalian expression vector pSecTag2 B (Invitrogen) between HindIII and BamHI restriction sites to express soluble proteins. pSecTag2 B vector has the IgK leader peptide on the N terminus and a Myc tag and His_6 tag on the C terminus. In addition, a full-length LRPIV was amplified using 129 bp of forward primer (which has Kozak sequence, start codon, tPA signal peptide sequence, and LRPIV sequence) and reverse primer with the HindIII restriction site and cloned into pcDNA3.3 TOPO vector (WT-LRPIV). Full-length LRPIV variants with glycine replacing aspartic acid residues 3354, 3394, 3556, 3595, 3633, and 3674 (Fig. 1*B*) in the calcium binding sites were made by site-directed mutagenesis using the QuikChange Lightning site-directed mutagenesis kit (Stratagene, LA Jolla, CA). WT-LRPIV was used as a template along with their respective primer sets.

Protein Expression—CHO cells were grown in CDOpti CHO medium supplemented with 1 mM $CaCl_2$ and 2 mM Glutamax at 37 °C in a shaker flask. The cells were then stably transfected with each construct using FreeStyle MAX reagent (Invitrogen). Five days after transfection, cells were grown into medium supplemented with 700 μg/ml Geneticin (for selection of cells with pcDNA 3.3 TOPO vector) or 200 μg/ml hygromycin (for selection of cells with pSecTag2 vector). After 12–15 days, around 5000 antibiotic-resistant cells were plated on a 100 × 10-mm Petri plate containing CloneMatrix (catalog no. K8510, Genetix Molecular Devices, Inc., Sunnyvale, CA) mixture (40% CloneMatrix, 50% 2× CDOpti CHO, and antibiotics). Three weeks after plating, 50–60 single clones were transferred into CDOpti CHO medium in 48-well plates. Three days later, media were collected and tested for expression of LRPIV by Western blot analysis. Selected clones were subsequently transferred into 12-well plates. A single selected clone was transferred into a Fernbach flask and grown as a suspension culture. Culture was started with 1×10^6/ml cell density in CDOpti CHO medium containing 2 mM Glutamax, 1 mM $CaCl_2$, and 10% CHO CD Efficient Feed A (Invitrogen). The cells were counted daily using a hemocytometer (Hausser Scientific Partnership, Horsham, PA), and glucose levels were determined using a GlucCell™ test strip (CESCO Bioengineering Co., Taichung, Taiwan). When the glucose level fell below 2 g/liter in the conditioned medium, cells were supplemented with 10% Feed A containing 2 mM Glutamax and 1 mM $CaCl_2$. After 10 days of culture, the conditioned medium was collected, centrifuged, filtered through 0.2-μm membrane, and stored frozen at −20 °C until analysis. The LRPIV-derived peptides CR25-CR26, CR26-CR27, CR25, CR26, and mutant proteins D3354G, D3595G, and D3633G were not included in the present study due to their poor secretion in the medium.

Purification of LRPIV Variants—Full-length LRPIV (CR21–CR31) and LRPIV CRs containing His_6 tag were purified using Ni^{2+}-nitrilotriacetic acid-agarose (Qiagen, Valencia, CA). Briefly, conditioned medium was mixed with 10% glycerol, 150 mM NaCl, 10 mM imidazole, and washed Ni^{2+}-nitrilotriacetic acid resin, rocked at room temperature for 30 min, and washed with a buffer (10% glycerol, 300 mM NaCl, 10 mM imidazole, and 50 mM NaH_2PO_4, pH 8). Bound protein was eluted with 250 mM imidazole in 50 mM phosphate buffer, pH 8. Eluted protein was passed through a 50-kDa cut-off filter (Millipore, Billerica, MA). The WT-LRPIV was purified by affinity purification using a GST-RAP affinity column as described (38). GST-RAP was expressed as reported (39) and affinity-purified using the B-PER GST fusion protein purification kit (Pierce). The GST-RAP affinity column was prepared using the AminoLink Plus immobilization kit (catalog no. 44894, Pierce). Mutant variants of LRPIV were purified using an anti-LRPIV-antibody affinity column. The anti-LRPIV-antibody column was prepared by immobilizing purified anti-LRPIV antibody (kindly provided by Dr. Komives) using the AminoLink Plus immobilization kit (Pierce). For purification of full-length LRPIV variants, about 100 ml of conditioned medium was diluted 3-fold with a wash buffer (20 mM Tris, 150 mM NaCl, pH 7.4) and loaded onto an anti-LRPIV antibody affinity column. The column was washed with 900 ml of wash buffer, and the bound protein was eluted with 0.1 M glycine buffer (pH 2.5), neutralized with 2 M Tris buffer (pH 9.5), and concentrated using a 10-kDa cut-off filter (Millipore). Each purified LRPIV variant was dialyzed against 50 mM carbonate-bicarbonate buffer (pH 9), and their purity was confirmed by silver staining (Fig. 1*C*). We screened eight LRPIV-derived peptides/proteins, which include LRPIV CRs (CR21–CR31, CR24–CR27, CR25–CR28, and CR25–CR27), WT-LRPIV, and full-length LRPIV variants (LRPIV-D3394G, LRPIV-D3556G, and LRPIV-D3674G) for their binding to Aβ40 and Aβ42 by ELISA.

In Vitro Binding Studies

Screening of LRPIV Variants for Ligand Binding by ELISA—Microtiter plates were coated with 5 μg/ml LRPIV analog overnight in 55 mM sodium bicarbonate buffer at 4 °C. All wells were blocked with protein-free buffer (catalog no. 37570, Pierce) for 1 h at room temperature. Varying concentrations of Aβ40, Aβ42, or ApoE2, -3, or -4 (catalog nos. P2002, P2003, and P2004, respectively, Invitrogen), tPA (catalog no. 10-633-45291, Genway Biotech, Inc., San Diego, CA), MMP-9 (catalog no. 911-MP-010, R&D Systems, Minneapolis, MN), and Factor IXa (catalog no. RP-43110, Pierce) were incubated in Hanks' balanced solution culture medium (HBSC), pH 7.4, containing 0.05% Tween 20 (HBSCT) at room temperature for 2 h. Anti-Aβ (1 μg/ml; catalog no. 2454, Cell Signaling Technology Inc.), anti-ApoE (0.1 μg/ml; catalog no. K74180, Biodesign Meridian LifeScience, Memphis, TN), anti-tPA (catalog no. Ab62763, Abcam, Cambridge, MA), anti-MMP-9 (catalog no. Ab5707, Abcam), or anti-Factor IXa (catalog no. LS-C23381, LifeSpan Biosciences, Inc., Seattle, WA) overnight at 4 °C in HBSCT containing 0.25% BSA. After washing plates four times with HBSCT, wells were incubated with goat anti rabbit-HRP or donkey anti-goat (1:3000 dilution) in HBSCT and 0.25% BSA for 30 min at room temperature. After washing plates four times with HBSCT, 100 μl of 3,3′,5,5′-tetramethylbenzidine substrate (catalog no. 53-00-01, KPL, Gaithersburg, MD) was

added. The reaction was developed for 10 min and stopped with 100 μl of 1 M HCl. The absorbance was read at 450 nm. To calculate the K_d (ligand concentration that binds to half of the microtiter plate immobilized LRPIV receptor sites at equilibrium), we utilized GraphPad Prism software (version 3) based on the Marquardt method of nonlinear one-site binding (hyperbola) regression (curve fit) analysis of the ELISA-based absorbance values against specific concentrations of the various ligands studied. GraphPad Prism software uses the following equation to calculate K_d: $Y = B_{max} \times X/(K_d + X)$, where B_{max} is the maximum specific binding in the same units as Y (Y is the specific binding extrapolated to very high concentrations of ligand, so its value is almost always higher than any specific binding measured in the experiment). K_d is the equilibrium binding constant, in the same units as X (X is the ligand concentration needed to achieve a half-maximum binding at equilibrium). We only measured LRP-bound ligand for the affinity calculation and did not measure free and unbound LRP constructs.

Characterization of Aβ Binding to LRPIV-D3674G by ELISA—The ELISA plates were coated with 10 μg/ml LRPIV-D3674G, and the plates were blocked with protein-free blocking buffer (catalog no. 37570, Pierce) as described (40). Aβ40 (100 nM) was prepared in HBSC, pH 7.4, for 2 h at room temperature. After washing with HBSC containing 0.05% Tween 20, an Aβ N terminus-specific antibody (1 μg/ml; catalog no. 2454, Cell Signaling), HRP-conjugated C terminus-specific antibody (BA27, WAKO ELISA kit), or non-immune IgG (NI-IgG) primary antibody was added and incubated overnight. The secondary detection antibody for the N terminus anti-Aβ antibody was goat anti-rabbit (1:2000 dilution; Dako). The reaction was developed with 3,3′,5,5′ tetramethylbenzidine (KPL) and stopped with 1 M HCl. Absorbance was read at 450 nM (40).

Characterization of LRPIV-D3674G Binding to Monomer, Oligomers, and Fibrils by a Dot Blot Assay—Oligomers and fibrils of Aβ40 were prepared as described earlier (41, 42) and confirmed by a dot blot assay using oligomer- and fibril-specific antibodies A11 and OC, respectively (41, 42). In the dot blot assay, 1 μg of Aβ40 monomers, oligomers, or fibrils was applied to a nitrocellulose membrane, and the membrane was blocked with protein-free blocking buffer (Pierce). The membrane was incubated with 10 μg/ml LRPIV-D3674G in HBSC, pH 7.4, for 2 h at room temperature, and the membrane was probed with a rabbit polyclonal anti-LRPIV antibody.

In Vivo Studies

Animals—C57Bl6 and *APPsw*$^{+/0}$ mice were purchased from Jackson Laboratories and Taconic Farms, respectively. Mice were housed under standard conditions (12-h light/dark cycle starting at 7:00 a.m.; 21 ± 2 °C; 55 ± 10% humidity) in solid bottomed cages on wood chip bedding. All studies were performed according to National Institutes of Health guidance using protocols approved by the University of Rochester Committee on Animal Resources. Mice were anesthetized by intraperitoneal injections with a mixture of ketamine (100 mg/kg) and xylazine (10 mg/kg).

Protein Radiolabeling—WT-LRP-IV and LRPIV-D3674G were radiolabeled with ^{125}I by the Pierce IODO-GEN® (catalog no. 28601, Thermo Scientific) method.

LRP-IV Pharmacokinetic Studies—Mice (C57BL6, 2–3 months old) were anesthetized as above, and a single bolus of ^{125}I-WT-LRP-IV or ^{125}I-LRPIV-D3674G in PBS was administered via femoral vein, and blood samples were collected from the retro-orbital sinus at different time points after injection within 24 h, as described earlier (14). Plasma samples were counted, and trichloroacetic acid (TCA)-precipitable radioactivity was determined. Pharmacokinetic parameters were determined using a non-compartmental intravenous bolus module of Kinetica version 5.1 software (Thermo Fisher Scientific).

Permeability Surface Area (PS) Product for LRPIV-D3674G and WT-LRPIV—^{125}I-WT-LRPIV (20 μCi/kg) or ^{125}I-LRPIV-D3674G (20 μCi/kg) was administered intravenously and compared with [^{14}C]sucrose (11 μCi/kg) uptake by the brain and CSF 1 h after injection of tracers. ^{125}I TCA-precipitable counts/min were determined in the plasma, CSF, and brain. In these studies, the brain was perfused briefly with cold PBS at the end of the experiment to remove residual vascular radioactivity, as confirmed by undetectable radioactivity of [^{14}C]sucrose (11 μCi/kg). The BBB PS product (μl/min/g) of [^{14}C]sucrose, ^{125}I-WT-LRPIV, and ^{125}I-LRPIV-D3674G was calculated by using the equation,

$$PS = [(V_D) \times C_{PL}(T)]/AUC \quad \text{(Eq. 1)}$$

where V_D is the volume of distribution of [^{14}C]sucrose, ^{125}I-WT-LRPIV, and ^{125}I-LRPIV-D3674G after 1 h of intravenous injection in whole brain homogenate; $C_{PL}(T)$ is the terminal plasma concentration of TCA-precipitable ^{125}I-WT-LRPIV, ^{125}I-LRPIV-D3674G, or [^{14}C]sucrose; and *AUC* is area under the curve on a plot of concentration *versus* time calculated as we described (43).

LRPIV Treatment of Wild Type Mice—Ten-week-old C57BL6 mice ($n = 5$ mice/group) were treated daily with WT-LRPIV or LRPIV-D3674G (20 μg/mouse, intravenously via the tail vein) or vehicle for 5 days. At the end of treatment, mice were sacrificed under anesthesia. Blood and CSF samples were collected, and plasma was immediately separated from blood at 4 °C. All samples were stored immediately at −80 °C. Mice were perfused intracardially with ice-cold heparinized saline and hemibrains homogenized in 2% SDS containing protease inhibitor mixture (Roche Applied Science). Mouse endogenous Aβ40 and Aβ42 levels in the plasma and brain were determined by mouse Aβ-specific ELISA as described below. WT-LRPIV and LRPIV-D3674G levels in CSF were determined by Western blot analysis as described earlier (14).

Mouse Aβ-specific ELISA—Briefly, for mouse Aβ40-specific sandwich ELISA, the capturing and biotinylated detecting antibodies were monoclonal mouse Aβ raised against amino acid residues 1–20 (catalog no. AMB0062, Invitrogen) and rabbit polyclonal anti-Aβ40 biotin conjugate (catalog no. 44-3489, Invitrogen), respectively. For mouse Aβ42-specific sandwich ELISA, the capturing and detecting antibody were AMB0062 and rabbit polyclonal anti-Aβ42 biotin conjugate (catalog no.

44-3449, Invitrogen), respectively. Murine synthetic Aβ40 and Aβ42 (American Peptide Co., Sunnyvale, CA) were used as standards, as reported (44).

Safety Studies

Plasma Cholesterol—Total cholesterol levels in plasma were determined using a kit (catalog no. 439-17501, Wako Chemicals USA Inc., Richmond, VA).

Mouse Plasma ApoE—Sandwich ELISA for murine plasma apoE was carried out as described (14). Plasma samples were diluted directly with BSAT-DPBS buffer (Dulbecco's phosphate-buffered saline (Cellgro, Mediatech, Inc.) with 5% BSA and 0.03% Tween 20, supplemented with complete protease inhibitor mixture (Roche Applied Science)). Pooled plasma from C57BL6 mice containing 68 μg/ml apoE was used as a standard as reported previously (14, 45). Briefly, 96-well plates (Costar, Corning) were coated overnight with 0.5 μg/well of the capturing antibody (catalog no. sc-6384, clone M-20, goat anti-mouse apoE, Santa Cruz Biotechnology, Inc., Santa Cruz, CA), blocked with 7% milk in PBS, and incubated with the secondary antibody, biotinylated goat anti-apoE (1:10,000 dilution, catalog no. K74180B, Biodesign Meridian LifeScience), followed by streptavidin-horseradish peroxidase conjugate (catalog no. SNN 2004, Invitrogen). The reaction was developed using 3,3′,5,5′-tetramethylbenzidine substrate (KPL), stopped with 1 N HCl, and quantified at 450 nm. The sensitivity of the assay was ~1 ng/ml.

Mouse Plasma tPA—Plasma levels of active mouse tPA were determined using a kit (catalog no. MTPAKT, Molecular Innovations, Novi, MI).

Mouse Plasma Pro-MMP-9—Plasma levels of mouse pro-MMP-9 were determined using a kit (Quantinine® MMP900, R&D Systems) and following the manufacturer's instructions.

Plasma Glucose Levels—Plasma glucose levels were determined using GlucCell™ Test Trip (CESCO, Bioengineering Co., Taichung, Taiwan).

Activated Partial Thromboplastin Time (aPTT)—Mouse blood samples were collected in citrate buffer (250 mM, pH 7.2) and centrifuged at 10,000 × *g* for 10 min to separate plasma. Plasma (25 μl) was incubated with 25 μl of TriniCLOT aPTT HS reagent (Trinity Biotech plc., Bray, Ireland) for 3 min at 37 °C in a Start4 coagulometer (Diagnostica Stago, Inc.). The aPTT reaction was started by adding 50 μl of 50 mM calcium chloride, and the time of clotting was recorded when the movement of the iron ball ceased under the magnetic field.

Lipoprotein Receptors and RAGE—Briefly, tissues were homogenized in Phosphosafe™ extraction buffer (catalog no. 71296, Novagen, EMD Millipore, Billerica, MA). Proteins were separated by SDS-PAGE and immunoblotted with an LRP1 light chain-specific antibody (catalog no. 438192, Calbiochem, EMD Millipore), anti-phosphotyrosine antibody (Sigma-Aldrich), low density lipoprotein receptor-specific antibody (catalog no. 15C8, Calbiochem, EMD Chemicals Inc.), and anti-RAGE antibody (catalog no. sc-5563, Santa Cruz Biotechnology, Inc.).

Western Blot Analysis—For detection of APP, frozen brain cortical tissues were homogenized in lysis buffer (Roche Applied Science) containing a complete protease inhibitor mixture (Roche Applied Science). The homogenate was centrifuged for 20 min at 20,000 × *g*. The supernatant was collected in a separate tube, and total protein concentration was determined by a BCA protein assay (Pierce). Brain lysate proteins were subjected to 4–12% NuPAGE BisTris SDS-PAGE (Invitrogen) and transferred to nitrocellulose membrane (Bio-Rad). Membrane was blocked with 5% nonfat milk in TBST for 1 h and incubated overnight with the primary monoclonal antibody against APP (MAB348, Chemicon, Temecula, CA). The membranes were washed and incubated with horseradish peroxidase-conjugated secondary antibody for 1 h. Immunoreactivity was detected using SuperSignal West Pico chemiluminescent substrate (Thermo Scientific).

CSF Levels of WT-LRPIV and LRPIV-D3674G—CSF samples (15 μl) were denatured in the SDS buffer by heating at 70 °C for 10 min. Samples were subjected to electrophoresis on an SDS-polyacrylamide gel and transferred to nitrocellulose. LRPIV was detected with a rabbit polyclonal anti-LRPIV antibody. In a separate experiment, ^{125}I TCA-precipitable counts in 20 μl of plasma and CSF were analyzed 1 h after a single bolus of ^{125}I-labeled WT-LRPIV or LRPIV-D3674G (20 μCi/kg) in PBS.

Immunogenicity Testing—Immunogenicity testing was outsourced (QED Bioscience Inc., San Diego, CA). Approximately 8–10-week-old BALB/c female mice (average weight 0.02 kg) were dosed (20, 40, and 60 μg/kg, intraperitoneally) four times biweekly. Retro-orbital blood samples of 250 μl each were collected before dosing and 1 week after following each injection. Each mouse was bled a total of five times. Blood samples were collected in heparinized tubes and centrifuged immediately after collection. Serum samples were frozen at −20 °C. After the last blood sample collection, all of the serum samples were tested for anti-LRPIV-D3674G antibody by ELISA. The plates were coated with three different LRPIV-D3674G concentrations (1, 5, or 20 μg/ml), and plasma samples were tested from 1:100 to 1:6400 dilutions for anti-LRPIV-D3674G antibodies. A rabbit LRPIV antiserum was used as a positive control.

LRPIV Treatment of APPsw$^{+/0}$ Mice—*APPsw*$^{+/0}$ mice ($n = 9$ mice/group) were treated subcutaneously with LRPIV-D3674G (40 μg/kg per day) or saline for 3 months beginning at the age of 6 months. After 3 months of treatment, we measured cerebral blood flow responses to brain activation by whisker stimulation and performed a burrowing behavioral test. After these functional tests, mice were sacrificed under anesthesia and brain, CSF, and plasma were collected and analyzed for human Aβ40 and Aβ42 levels as described earlier (14).

Burrowing Test—*APPsw*$^{+/0}$ mice after 3 months of treatment with LRPIV-D3674G were subjected to a burrowing behavior test. The burrowing test was performed as described (46). Briefly, mice were individually placed in the cages equipped with a burrow made from a 200-mm-long, 68-mm-diameter tube of PVC plastic. One end of the tube was closed by a PVC cap. The open end of the tube was raised ~30 mm by a PVC ring. The burrow was filled with 200 g of mouse food pellets, and the mice were allowed to burrow for 3 h. The weight of the remaining food pellets inside the burrow was determined to obtain a measurement of the amount burrowed.

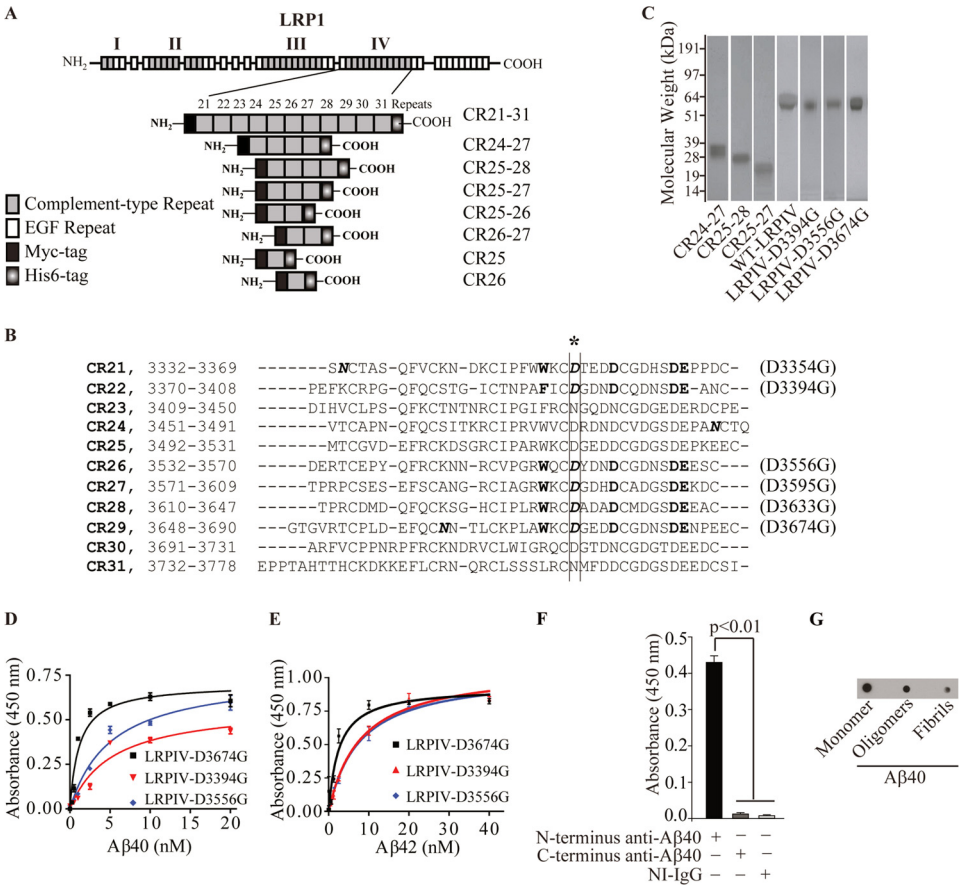

FIGURE 1. **Generation of recombinant LRPIV-derived proteins/peptides and binding of Aβ40 and Aβ42 to novel LRPIV-derived mutants *in vitro*.** *A*, schematic diagram showing four ligand binding domains of LRP1 (clusters I, II, III, and IV) consisting of CR2, CR8, CR10, and CR11, respectively. Full-length LRPIV of 11 repeats (CR21–CR31) and seven fragments of LRPIV (CR24–CR27, CR25–CR28, CR25–CR27, CR25–CR26, CR26–CR27, CR25, and CR26) were secreted by CHO cells as Myc- and His_6-tagged soluble proteins after transfection with respective plasmid constructs. *B*, LRPIV amino acid sequence (3332–3778; accession number NM_002332) showing regions for the complement-type repeats. The amino acid residues involved in calcium binding are shown in *boldface type*. The aspartic acid residues in italic type (*) are replaced with glycine by site-directed mutagenesis to generate LRPIV variants. *C*, representative silver staining of the purified recombinant LRPIV-derived peptides/proteins used for Aβ binding studies. *D* and *E*, binding curves for human Aβ40 and Aβ42 to immobilized LRPIV mutants obtained by ELISAs, $n = 3$ assays/group. Binding constants (K_d) were calculated from corresponding binding curves (see Tables 2 and 3 and "Experimental Procedures" for details). *F*, Aβ binding to immobilized LRPIV-D3674G in the presence of an Aβ N terminus-specific antibody, C terminus-specific antibody, or non-immune IgG (*NI-IgG*). *G*, binding of LRPIV-D3674G to immobilized Aβ monomers, oligomers, and fibrils by a dot blot assay. *Error bars*, S.E.

Microglia—Formaldehyde fixed brain sections were used for immunostaining of the microglia marker Iba-1 (ionized calcium-binding adaptor molecule 1), as described (47).

Prussian Blue Staining—Briefly, acetone-fixed saggital brain sections from vehicle-treated and LRPIV-D3674-treated mice were incubated in a 5% potassium ferrocyanide and 5% hydrochloric acid solution (1:1 working solution) for 30 min, as reported (48). Hemosiderin shows a blue color. To analyze the abundance of Prussian blue-positive deposits per section, the total numbers of Prussian blue-positive spots were divided by the number of sections analyzed.

Statistical Analysis—The results were compared by one-way multifactorial analysis of variance followed by Tukey's post hoc analysis for more than two groups of data or Student's *t* test for unpaired data of two groups. The differences were considered to be significant at $p < 0.05$. All values are mean ± S.E.

RESULTS

Generation of Recombinant LRPIV-derived Analogs—We generated eight recombinant CR fragments of LRPIV with Myc and His_6 tags (*i.e.* CR24–CR27, CR25–CR28, CR25–CR27, CR25–CR26, CR26-CR27, CR25, CR26, and CR21–CR31, corresponding to full-length LRPIV (Fig. 1, *A* and *B*). We also generated WT-LRPIV without Myc and His_6 tags or the 16-amino acid peptide tag derived from factor VIII (tagged WT-LRPIV) that has been described previously (38, 49, 50). Two single CRs (CR25 and CR26), two double CRs (CR25-CR26 and CR26-CR27), and CR21–CR31 were eliminated from further screening because of their poor secretion by CHO cells into the medium. The remaining three LRPIV fragments were purified from CHO-secreted medium, including two four-CR fragments (CR24–CR27 and CR25–CR28) and one three-CR fragment (CR25–CR27), and, along with the full-length WT-LRPIV (Fig. 1*C*), were used for the binding studies. We set the criterion that a lead analog has to have a higher binding affinity for both Aβ40 and Aβ42 (*i.e.* lower K_d value) compared with previously described tagged WT-LRPIV, which has been shown to bind Aβ40 and Aβ42 *in vitro* with K_d values of 2 and 5 nM, respectively (14). The K_d for Aβ40 binding to CHO-secreted WT-LRPIV was 1.90 ± 0.40 nM (Table 2), which was comparable

TABLE 2

K_d values for Aβ binding to WT-LRPIV, LRPIV CRs, and LRPIV full-length variants with aspartic acid replaced with glycine in the calcium-binding sites

Values are means ± S.E., $n = 3$ assays/group.

CRs and LRPIV full-length variants	K_d Aβ40	K_d Aβ42
	nM	
CR24–CR27	6.5 ± 2.3	4.1 ± 0.8
CR25–CR28	12.9 ± 2.6	4.0 ± 0.7
CR25–CR27	13.6 ± 2.3	4.1 ± 0.7
WT-LRPIV	1.9 ± 0.4	6.8 ± 1.5
LRPIV-D3674G	1.2 ± 0.2[a]	2.5 ± 0.6[a]
LRPIV-D3394G	5.2 ± 1.1	7.8 ± 1.1
LRPIV-D3556G	5.1 ± 1.1	7.6 ± 0.9

[a] $p < 0.05$, Aβ binding affinity to LRPIV-D3674 was significantly higher compared with WT-LRPIV or any other studied LRPIV analog.

with K_d for Aβ40 binding to tagged WT-LRPIV produced by the baby hamster kidney cell line (14). However, Aβ40 bound with 3.5–7-fold lower affinity to CR24–CR27, CR25–CR28, and CR25–CR27 than to WT-LRPIV (Table 2) or tagged WT-LRPIV (14), which eliminated these CRs from further screening, although Aβ42 binding to these CRs was somewhat improved relative to WT-LRPIV (Table 2) and/or tagged WT-LRPIV (14).

Next, we performed site-directed mutagenesis, replacing the aspartic acid residue with glycine in the calcium binding sites of CR21, CR22, CR26, CR27, CR28, and CR29 and generated six full-length LRPIV mutants (*i.e.* D3354G, D3394G, D3556G, D3595G, D3633G, and D3674G, respectively) (Fig. 1*B*). Three LRPIV mutants (D3354G, D3585G, and D3633G) were eliminated from screening because of low levels of secreted protein. The remaining three LRPIV analogs, including the D3394G, D3556G, and D3674G LRPIV variants, were purified (Fig. 1*C*) and screened. LRPIV-D3674G mutant bound Aβ40 and Aβ42 with the highest affinity with a K_d of 1.20 ± 0.18 and 2.51 ± 0.6 nM, respectively, indicating 3–4-fold better affinity for the respective Aβ peptides than D3394G or D3556G mutants (Fig. 1, *D* and *E*, and Table 2). Importantly, compared with WT-LRPIV or tagged WT-LRPIV (14), LRPIV-D3674G bound Aβ40 and Aβ42 with ~1.6- and 2.7-fold greater affinity, respectively (Table 2) and therefore met our criterion for a lead Aβ-binding LRPIV analog.

To determine which region of Aβ is recognized by LRPIV-D3674G, we have studied *in vitro* binding of Aβ40 to immobilized LRPIV-D3674G with and without N terminus anti-Aβ40, C terminus anti-Aβ40, and control NI-IgG antibodies (Fig. 1*F*). This experiment has shown that LRPIV-D3674G binds to the C-terminal sequence of Aβ, which is consistent with a previous report showing that the wild type form of recombinant LRP-IV containing an extraneous 16-amino acid "tag," which contains the antigenic determinant of the mouse monoclonal antibody CLB-CAg 69 against Factor VIII (35, 51), also binds the Aβ C-terminal domain (40). The precise amino acid sequence that LRPIV-D3674G detects will be determined by future epitope mapping studies. We also show that LRPIV-D3674G can bind, in addition to Aβ monomers, also Aβ oligomers and Aβ fibrils (Fig. 1*G*).

Because LRPIV binds multiple ligands besides Aβ, we studied binding of different LRP1 ligands for WT-LRPIV and LRPIV-D3674G, a lead new LRPIV analog, to determine whether LRPIV-D3674G mutation increases or decreases binding of other LRP1 ligands. Compared with WT-LRPIV, LRPIV-D3674G bound apoE2, apoE3, apoE4, tPA, MMP-9, and factor IXa, with ~1.3–4.1-fold lower affinity (Table 3). These data indicate that the LRPIV-D3674G mutation also improves Aβ binding relative to other studied LRP1 ligands.

TABLE 3

K_d values for LRP1 ligands binding to WT-LRPIV and LRPIV-D3674G

Values are means ± S.E., $n = 3$ assays/group.

Ligands	WT-LRPIV K_d	LRPIV-D3674G K_d	LRPIV-D3674G/WT-LRPIV K_d ratio
	nM	nM	
APOE2	24.4 ± 1.9	40.8 ± 2.6[a]	1.6
APOE3	29.3 ± 2.1	54.3 ± 6.4[a]	1.8
APOE4	39.5 ± 3.2	49.9 ± 5.4[a]	1.3
tPA	106.3 ± 20.7	284.5 ± 35.0[a]	2.7
MMP-9	141.2 ± 25.5	575.3 ± 137.3[a]	4.1
Factor IXa	158.3 ± 10.3	601.9 ± 40.2[a]	3.8

[a] $p < 0.05$. The difference in K_d values between WT-LRPIV and LRPIV-D3674G was considered to be significant at $p < 0.05$.

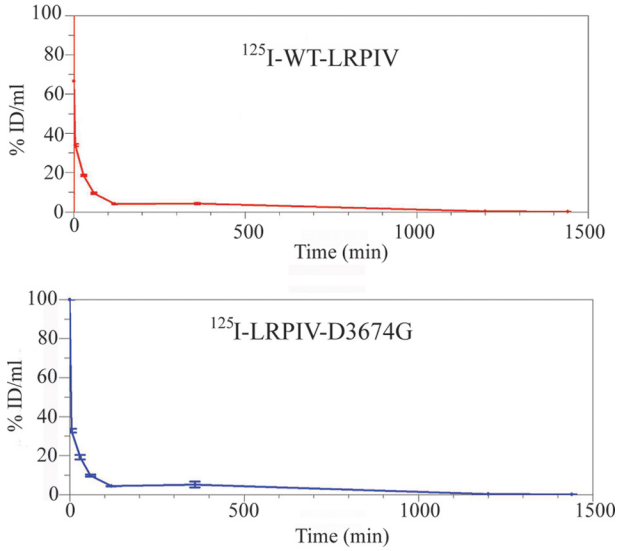

FIGURE 2. **Plasma profile of TCA-precipitable ^{125}I-WT-LRPIV and ^{125}I-LRPIV-D3674G activity within 24 h of intravenous administration expressed as a percentage of the injected dose/ml of plasma (% *ID/ml*).** Values are mean ± S. E., $n = 3$ mice/group.

TABLE 4

Pharmacokinetic parameters for WT-LRPIV and LRPIV-D3674G

Values are means ± S.E., $n = 3$ assays/group.

Parameter	WT-LRPIV	LRPIV-D3674G
$t_{½}$ (min)	206.6 ± 3.9	208.0 ± 3.8[a]
Mean residence time (min)	284.3 ± 3.7	288.0 ± 12.1[a]
Area under curve (min × % injected dose/ml)	3907.3 ± 85.9	4147.6 ± 249.4[a]

[a] Not significant.

Plasma Elimination of WT-LRPIV and LRPIV-D3674G—There was no significant difference in the systemic clearance rate ($t_{½}$ ~3.4 h) or mean residence time (~4.8 h) of ^{125}I-WT-LRP-IV or ^{125}I-LRPIV-D3674G after an intravenous injection of tracers (Fig. 2 and Table 4). However, the $t_{½}$ was shorter compared with previously reported $t_{½}$ for the wild type form of recombinant LRP-IV containing an extraneous 16-amino acid tag, which contains the antigenic determinant of the mouse monoclonal antibody CLB-CAg 69 against Factor VIII used to

purify the peptide from the culture medium (14). It remains unclear how the Factor VIII tag prolongs the rate of systemic clearance of WT-LRP-IV ($t_{½}$ = 11.8 h) (14), but it is of note that none of the presently studied forms of LRP-IV contained this extraneous 16-amino acid tag of Factor VIII.

Clearance of Mouse Endogenous Brain Aβ by LRPIV-D3674G—Five-day intravenous treatment of C57Bl6 mice (20 μg/mouse) with WT-LRPIV or LRPIV-D3674G at a dose comparable with that used previously to treat C57Bl6 mice with tagged WT-LRPIV (14) significantly reduced mouse endogenous brain Aβ levels. For example, compared with vehicle, LRPIV-D3674G mutant lowered brain Aβ40 and Aβ42 levels by 42 and 45%, respectively (Fig. 3, *A* and *B*), which correlated with the corresponding increases in total plasma levels of Aβ40 and Aβ42 (Fig. 3, *C* and *D*), most of which was bound to the LRPIV-D3674G mutant (not shown), similar to what was reported previously for tagged WT-LRPIV in C57Bl6 mice treated with tagged WT-LRPIV (14). Compared with WT-LRPIV, LRPIV-D3674G was more efficacious in removing mouse endogenous brain Aβ, as indicated by ~25 and 27% greater reductions in brain Aβ40 and Aβ42 levels compared with the respective Aβ peptide reductions with WT-LRPIV (Fig. 2, *A* and *B*).

LRPIV-D3674G Does Not Affect Activity of Other LRP1 Ligands in Mice—We analyzed plasma and tissue samples from C57Bl6 mice treated intravenously with 20 μg of LRPIV-D3674G/mouse daily for potential side effects. LRPIV-D3674G did not alter plasma levels of cholesterol, glucose, or LRP1 ligands, such as apoE, tPA, and pro-MMP-9 (Fig. 4, *A–E*). Plasma clotting time determined by the aPTT remained unchanged within 2 h of intravenous LRPIV-D3674G administration (Fig. 4*F*). In liver and brain microvessels, there were no changes in the expression levels of low density lipoprotein receptor or LRP1 (Fig. 5, *A* and *B*). In addition, in the brain, there were no changes in phosphorylated LRP1 levels after LRPIV-D3674G treatment (Fig. 5*C*). Expression of RAGE, an Aβ influx transporter (4), was not altered in brain microvessels by LRPIV-D3674G treatment (Fig. 5*D*). Furthermore, APP levels in the brain were not altered by LRPIV-D3674G treatment (Fig. 5*E*). LRPIV-D3674G did not enter CSF (Fig. 5*F*), similar to tagged WT-LRPIV (14), suggesting that its action is on sequestering the peripheral Aβ pool. Using radiolabeled ^{125}I-WT-LRPIV and ^{125}I-LRPIV-D3674G, we have independently confirmed that neither peptide is transported into the CSF and brain, as determined by non-detectable radioactivity in the CSF and non-detectable PS products for either form of LRP-IV (Fig. 5, *G* and *H*). For immunogenicity testing, blood samples were collected at the time of antigen administration and 1, 3, 5, and 7 weeks afterward. Antibodies to LRPIV-D3674G were not detected in postimmunization plasma samples in mice after treatment with increasing doses of LRPIV-D3674G, as described under "Experimental Procedures" (Fig. 5*I*).

LRPIV-D3674G Treatment of APPsw$^{+/0}$ Mice—Compared with vehicle-treated *APPsw*$^{+/0}$ mice, *APPsw*$^{+/0}$ mice treated daily with a subcutaneous low dose of LRPIV-D3674G (40 μg/kg) for 3 months beginning at 6 months of age showed significant reductions of Aβ40 and Aβ42 levels in hippocampus, cortex, and CSF by 60–80% (Fig. 6, *A–D*), as determined at 9 months of age. As expected, LRPIV-D3674G treatment significantly increased plasma Aβ40 and Aβ42 levels (Fig. 6, *E* and *F*). Treatment with LRPIV-D3674G also increased cerebral blood flow (CBF) responses to whisker stimulation by 75% (Fig. 6*G*) and significantly improved hippocampal function compared with vehicle-treated mice, as indicated by the burrowing test showing an approximately 60% improvement (Fig. 6*H*). The LRPIV-D3674 treatment in *APPsw*$^{+/0}$ mice did not influence inflammatory response and did not increase microhemorrhages, as shown by non-significant differences in the number of Iba1-positive microglia (Fig. 7, *A* and *B*) and Prussian blue-positive hemosiderin deposits (Fig. 7, *C* and *D*) in LRPIV-D3674-treated compared with vehicle-treated animals.

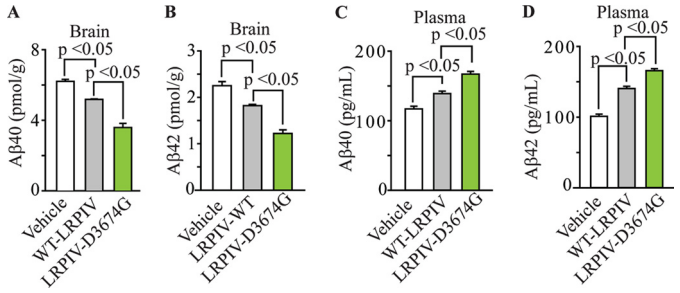

FIGURE 3. **LRPIV-D3674G clears mouse endogenous brain Aβ more efficiently than WT-LRPIV in C57BL/6 mice.** Shown are brain levels (*A* and *B*) and total plasma levels (*C* and *D*) of Aβ40 and Aβ42 in vehicle-treated (*white*), WT-LRPIV-treated (*gray*), and LRPIV-D3674G-treated (*green*) mice (intravenously for 5 days, 20 μg/day/mouse). Values are mean ± S.E. (*error bars*), n = 3–5 mice/group. The differences were considered to be significant at $p < 0.05$.

DISCUSSION

Plasma sLRP1 levels are reduced in AD and MCI-AD patients, and sLRP1 is oxidized, which results in diminished Aβ

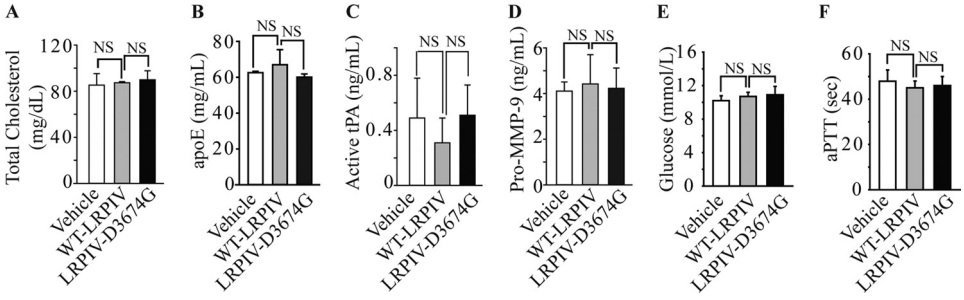

FIGURE 4. **Plasma levels of total cholesterol (*A*), mouse endogenous apoE (*B*), activated mouse tPA (*C*), mouse pro-MMP-9 (*D*), and glucose (*E*) and aPTT (*F*) in C57BL6 mice treated with vehicle, WT-LRPIV, or LRPIV-D3674G (intravenously for 5 days, 20 μg/day).** Values are means ± S.E. (*error bars*), n = 3 mice/group. *NS*, non-significant.

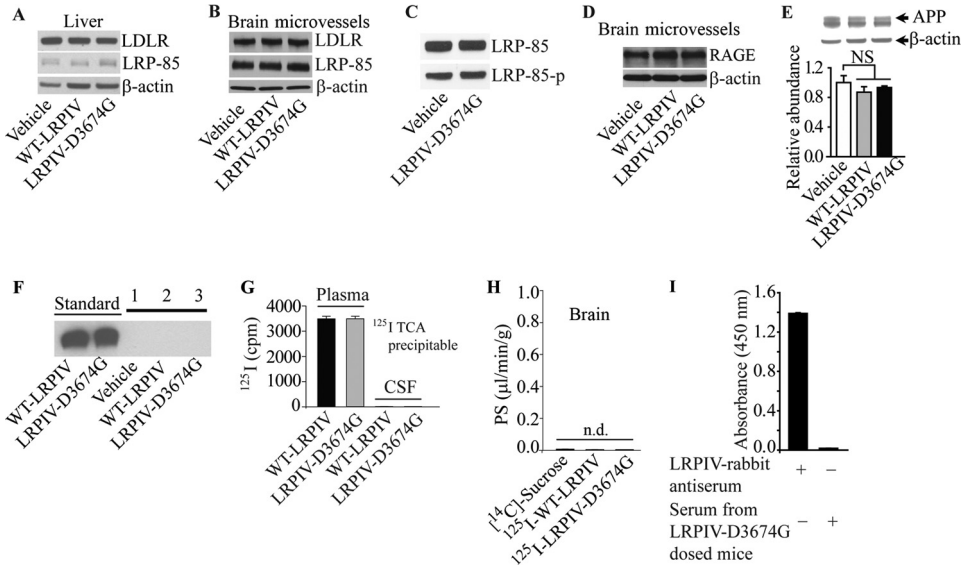

FIGURE 5. *A–F*, representative Western blot analysis of low density lipoprotein receptor and LRP1 in liver (*A*) and brain microvessels (*B*), phosphorylated LRP1 in brain (*C*), RAGE in brain microvessels (*D*), brain APP levels (*E*), and undetectable CSF levels of WT-LRPIV and LRPIV-D3674G in the CSF (*F*) in mice treated with vehicle, WT-LRPIV, or LRPIV-D3674G (intravenously for 5 days, 20 μg/day). *G*, ^{125}I TCA-precipitable counts/min (cpm) in plasma and CSF. *H*, the PS product showing non-detectable (*n.d.*) TCA-precipitable ^{125}I-WT-LRPIV and ^{125}I-LRPIV-D3674G brain uptake 1 h after intravenous injections of these peptides at (20 μCi/kg compared with [^{14}C]sucrose (11 μCi/kg). Values are means ± S.E. (*error bars*), $n = 3$ mice/group. *I*, undetectable antibodies to LRPIV-D3674G in plasma of mice treated with LRPIV-D3674G (40 μg/kg, intraperitoneally) for 3 months. *NS*, non-significant.

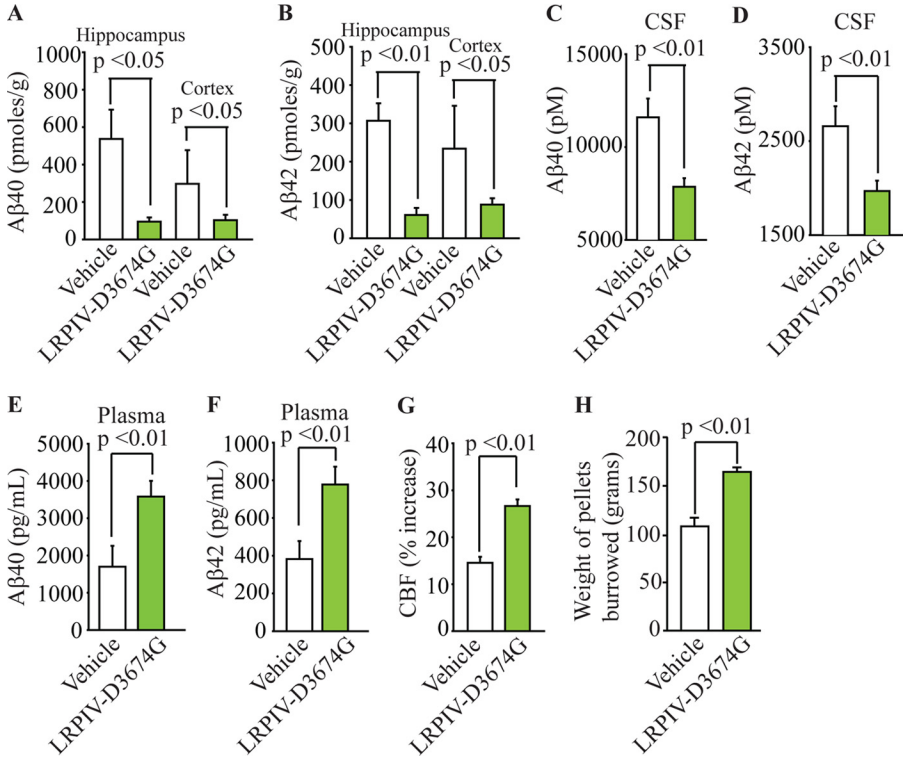

FIGURE 6. **LRPIV-D3674G clears human brain Aβ and improves function in *APPsw*$^{+/0}$ mice.** LRPIV-D3674 was administered subcutaneously, 40 μg/kg body weight/day, for 3 months beginning at 6 months of age. Shown are brain (hippocampus and cortex) levels (*A* and *B*), cerebrospinal fluid levels (*C* and *D*), and plasma levels (*E* and *F*) of Aβ40 and Aβ42 in vehicle-treated (*white*) and LRPIV-D3674G-treated (*green*) *APPsw*$^{+/0}$ mice. *G*, percentage increase in CBF in response to whisker stimulation in vehicle-treated (*white*) and LRPIV-D3674G-treated (*green*) *APPsw*$^{+/0}$ mice. *H*, weight of pellets burrowed in vehicle-treated (*white*) and LRPIV-D3674G-treated (*green*) *APPsw*$^{+/0}$ mice. Values are mean ± S.E. (*error bars*), $n = 6–9$ mice/group. The differences were considered to be significant at $p < 0.05$.

peripheral binding and higher levels of free Aβ in plasma (14, 22). In addition, WT-LRPIV binds free Aβ in plasma of AD patients (14). Experimental studies have shown that free Aβ re-enters the brain (4, 23, 24, 52) and that sLRP1 and/or its recombinant LRPIV ligand binding domain prevent plasma Aβ from entering the brain (14). These studies underscored the need for development of sLRP1 replacement therapy for AD to maintain low levels of free, unbound Aβ in plasma and restore

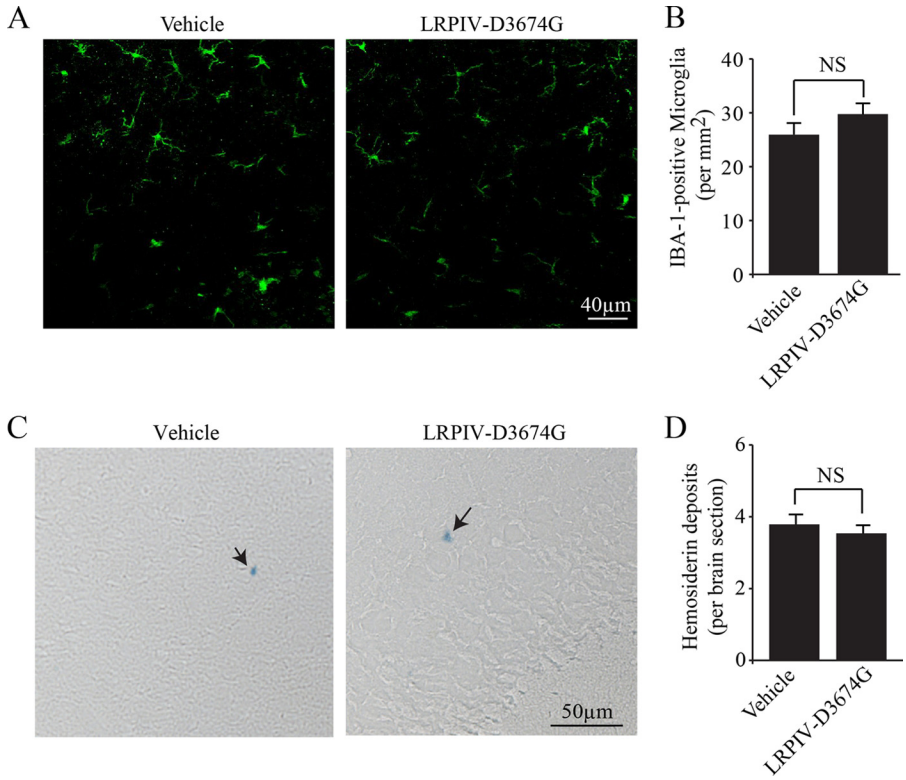

FIGURE 7. *A–D*, confocal microscopy analysis of Iba1-positive microglia (*green*) (*A*), the number of Iba1-positive microglia/mm^2 in the cortex (*B*), Prussian blue staining for hemosiderin in sagittal brain sections (*C*), and the total number of hemosiderin deposits per sagittal brain section (*D*) in *APPsw*$^{+/0}$ mice treated subcutaneously with LRPIV-D3674G (40 μg/kg per day) or vehicle for 3 months beginning at 6 months of age. Values are mean ± S.E. (*error bars*), $n = 3$ mice/group; *NS*, non-significant.

an important homeostatic mechanism regulating brain Aβ (11). Circulating endogenous Aβ antibodies that bind a fraction of Aβ in plasma (14, 22, 53–56) are also decreased in early stages of AD (22, 57, 58), further emphasizing the need for peripheral Aβ binding treatments. Peripheral Aβ-binding agents, such as Aβ antibodies (25, 48, 59–61), gelsolin (62, 63), soluble RAGE (4), and LRPIV (14), have been shown to promote Aβ clearance from the brain, reducing brain Aβ and amyloid load in different *APP*-overexpressing mice.

LRP1 at the BBB, sLRP1 in plasma, and LRP1 in the liver have important roles in homeostasis of brain Aβ (5). Down-regulation of LRP1 at the BBB due to vascular risk factors and/or oxidative stress (17, 64), oxidation, or reduced levels of sLRP1 in plasma (14) and reduced expression of LRP1 in the liver (65) lead to accumulation of Aβ in brain in different experimental models. A novel recombinant LRPIV-D3674G variant described here preferentially binds Aβ compared with other ligands and effectively reduces Aβ brain levels in wild type mice and AD mice without noticeable side effects. Moreover, treatment with LRPIV-D3674G increased CBF responses to whisker stimulation in AD mice. Whether the improved CBF responses contribute to reductions in Aβ levels in the brain by promoting Aβ clearance into cerebral circulation remains to be determined by future studies designed to measure Aβ clearance and production under experimentally different CBF conditions. LRPIV-D3674G did not enter CSF or brain, which is not unexpected because WT-LRPIV also does not cross the BBB (14), and peptides and proteins in general need specific transport systems expressed in brain endothelium for their transport into the brain (66).

The data presented here represent the first screening of LRPIV-derived analogs for Aβ binding. LRPIV has been shown to bind a range of functionally distinct ligands (35, 37, 38, 49). The surface plasmon resonance analysis has shown that the CR24–CR28 LRPIV region most effectively binds RAP, α_2M*, Factor VIII light chain, and Factor IXa (35). The three triple repeats, CR24–CR26, CR25–CR27, and CR26–CR28, interact avidly with RAP compared with the other CRs of LRPIV (33). Although the Aβ binding site on LRPIV has not been characterized, it seems plausible that this site might overlap partially or fully with the RAP binding site(s) because we have previously shown that RAP abolishes Aβ binding to LRPIV (8). Although Aβ40 and Aβ42 interacted with all studied CR fractions (CR24–CR27, CR25–CR28, and CR25–CR27), their binding affinities varied. In contrast to Aβ42, full-length WT-LRPIV was required for high affinity binding of Aβ40. Other studies have reported that CR24–CR26 is involved in high affinity binding of α_2M* and Factor VIII light chain (35). Site-directed mutation at a calcium binding site within CR29 (D3674G) increased the affinity for Aβ (Aβ42 > Aβ40) but decreased the affinity for other studied LRP1 ligands, whereas mutations within CR22 (D3394G) and CR26 (D3556G) reduced their respective binding affinities for both Aβ40 and Aβ42.

Calcium is required for proper folding and structural stability of the CR regions (33). The calcium ion binding requires the side chain of four acidic residues and two carbonyl groups, usu-

ally an aspartate residue and an aromatic residue. These two residues are involved in ligand interaction with LRP1 (67, 68). CRs (CR23, CR30, and CR31) with imperfect calcium coordination have reduced ligand-binding affinities (35). Also, calcium is required for binding of some LRP1 ligands, such as RAP and α_2M* (37), but not for other LRP1 ligands, such as apoE and lactoferrin (37). Importantly, mutation in CR29 resulted in conformational change in LRPIV, which enhanced binding of Aβ, especially Aβ42, but reduced binding of other ligands, including apoE2, apoE3, apoE4, tPA, MMP-9, and Factor IXa. The nature of the conformational change in the LRPIV-D3674G variant and mechanism of the enhanced Aβ binding will require future structural and biophysical studies.

In summary, we have demonstrated that LRPIV-D3674G exhibits significantly improved Aβ binding compared with WT-LRPIV. Moreover, LRPIV-D3674G efficiently cleared Aβ from the brain in wild type and AD mice. In addition, our data show that LRPIV-D3674G binds with reduced affinity several studied LRP1 ligands *in vitro* and does not affect noticeably their activity *in vivo* in mice. Therefore, LRPIV-D3674G could be developed as a potential therapeutic agent administered as a monotherapy and/or in combination with other Aβ-lowering agents, such as Notch-sparing γ-secretase inhibitors or β-secretase (BACE1) inhibitors (57, 69, 70) to restore the natural peripheral sink mechanism for Aβ in MCI and AD patients (22, 71).

Acknowledgments—We thank Dr. R. Deane for helpful discussions and M. Watrobski for skillful technical assistance.

REFERENCES

1. Querfurth, H. W., and LaFerla, F. M. (2010) Alzheimer's disease. *N. Engl. J. Med.* **362,** 329–344
2. Selkoe, D. J. (2001) Alzheimer's disease. Genes, proteins, and therapy. *Physiol. Rev.* **81,** 741–766
3. Benilova, I., Karran, E., and De Strooper, B. (2012) The toxic Aβ oligomer and Alzheimer's disease. An emperor in need of clothes. *Nat. Neurosci.* **15,** 349–357
4. Deane, R., Du Yan, S., Submamaryan, R. K., LaRue, B., Jovanovic, S., Hogg, E., Welch, D., Manness, L., Lin, C., Yu, J., Zhu, H., Ghiso, J., Frangione, B., Stern, A., Schmidt, A. M., Armstrong, D. L., Arnold, B., Liliensiek, B., Nawroth, P., Hofman, F., Kindy, M., Stern, D., and Zlokovic, B. (2003) RAGE mediates amyloid-β peptide transport across the blood-brain barrier and accumulation in brain. *Nat. Med.* **9,** 907–913
5. Zlokovic, B. V., Deane, R., Sagare, A. P., Bell, R. D., and Winkler, E. A. (2010) Low-density lipoprotein receptor-related protein-1. A serial clearance homeostatic mechanism controlling Alzheimer's amyloid β-peptide elimination from the brain. *J. Neurochem.* **115,** 1077–1089
6. Mawuenyega, K. G., Sigurdson, W., Ovod, V., Munsell, L., Kasten, T., Morris, J. C., Yarasheski, K. E., and Bateman, R. J. (2010) Decreased clearance of CNS β-amyloid in Alzheimer's disease. *Science* **330,** 1774
7. Shibata, M., Yamada, S., Kumar, S. R., Calero, M., Bading, J., Frangione, B., Holtzman, D. M., Miller, C. A., Strickland, D. K., Ghiso, J., and Zlokovic, B. V. (2000) Clearance of Alzheimer's amyloid-ss(1–40) peptide from brain by LDL receptor-related protein-1 at the blood-brain barrier. *J. Clin. Invest.* **106,** 1489–1499
8. Deane, R., Wu, Z., Sagare, A., Davis, J., Du Yan, S., Hamm, K., Xu, F., Parisi, M., LaRue, B., Hu, H. W., Spijkers, P., Guo, H., Song, X., Lenting, P. J., Van Nostrand, W. E., and Zlokovic, B. V. (2004) LRP/amyloid β-peptide interaction mediates differential brain efflux of Aβ isoforms. *Neuron* **43,** 333–344
9. Ito, S., Ohtsuki, S., and Terasaki, T. (2006) Functional characterization of the brain-to-blood efflux clearance of human amyloid-β peptide (1–40) across the rat blood-brain barrier. *Neurosci. Res.* **56,** 246–252
10. Saido, T., and Leissring, M. A. (2012) Proteolytic degradation of amyloid β-protein. *Cold Spring Harb. Perspect. Med.* **2,** a006379
11. Zlokovic, B. V. (2011) Neurovascular pathways to neurodegeneration in Alzheimer's disease and other disorders. *Nat. Rev. Neurosci.* **12,** 723–738
12. Banks, W. A., Robinson, S. M., Verma, S., and Morley, J. E. (2003) Efflux of human and mouse amyloid β proteins 1–40 and 1–42 from brain. Impairment in a mouse model of Alzheimer's disease. *Neuroscience* **121,** 487–492
13. Bell, R. D., Sagare, A. P., Friedman, A. E., Bedi, G. S., Holtzman, D. M., Deane, R., and Zlokovic, B. V. (2007) Transport pathways for clearance of human Alzheimer's amyloid β-peptide and apolipoproteins E and J in the mouse central nervous system. *J. Cereb. Blood Flow Metab.* **27,** 909–918
14. Sagare, A., Deane, R., Bell, R. D., Johnson, B., Hamm, K., Pendu, R., Marky, A., Lenting, P. J., Wu, Z., Zarcone, T., Goate, A., Mayo, K., Perlmutter, D., Coma, M., Zhong, Z., and Zlokovic, B. V. (2007) Clearance of amyloid-β by circulating lipoprotein receptors. *Nat. Med.* **13,** 1029–1031
15. Deane, R., Sagare, A., Hamm, K., Parisi, M., Lane, S., Finn, M. B., Holtzman, D. M., and Zlokovic, B. V. (2008) apoE isoform-specific disruption of amyloid β peptide clearance from mouse brain. *J. Clin. Invest.* **118,** 4002–4013
16. Jaeger, L. B., Dohgu, S., Hwang, M. C., Farr, S. A., Murphy, M. P., Fleegal-DeMotta, M. A., Lynch, J. L., Robinson, S. M., Niehoff, M. L., Johnson, S. N., Kumar, V. B., and Banks, W. A. (2009) Testing the neurovascular hypothesis of Alzheimer's disease. LRP-1 antisense reduces blood-brain barrier clearance, increases brain levels of amyloid-β protein, and impairs cognition. *J. Alzheimers Dis.* **17,** 553–570
17. Bell, R. D., Deane, R., Chow, N., Long, X., Sagare, A., Singh, I., Streb, J. W., Guo, H., Rubio, A., Van Nostrand, W., Miano, J. M., and Zlokovic, B. V. (2009) SRF and myocardin regulate LRP-mediated amyloid-β clearance in brain vascular cells. *Nat. Cell Biol.* **11,** 143–153
18. Sehgal, N., Gupta, A., Valli, R. K., Joshi, S. D., Mills, J. T., Hamel, E., Khanna, P., Jain, S. C., Thakur, S. S., and Ravindranath, V. (2012) *Withania somnifera* reverses Alzheimer's disease pathology by enhancing low-density lipoprotein receptor-related protein in liver. *Proc. Natl. Acad. Sci. U.S.A.* **109,** 3510–3515
19. Sagare, A. P., Deane, R., and Zlokovic, B. V. (2012) Low-density lipoprotein receptor-related protein 1. A physiological Aβ homeostatic mechanism with multiple therapeutic opportunities. *Pharmacol. Ther.* **136,** 94–105
20. Qosa, H., Abuznait, A. H., Hill, R. A., and Kaddoumi, A. (2012) Enhanced brain amyloid-β clearance by rifampicin and caffeine as a possible protective mechanism against Alzheimer's disease. *J. Alzheimers Dis.* **31,** 151–165
21. Kanekiyo, T., Liu, C. C., Shinohara, M., Li, J., and Bu, G. (2012) LRP1 in brain vascular smooth muscle cells mediates local clearance of Alzheimer's amyloid-β. *J. Neurosci.* **32,** 16458–16465
22. Sagare, A. P., Deane, R., Zetterberg, H., Wallin, A., Blennow, K., and Zlokovic, B. V. (2011) Impaired lipoprotein receptor-mediated peripheral binding of plasma amyloid-β is an early biomarker for mild cognitive impairment preceding Alzheimer's disease. *J. Alzheimers Dis.* **24,** 25–34
23. Ujiie, M., Dickstein, D. L., Carlow, D. A., and Jefferies, W. A. (2003) Blood-brain barrier permeability precedes senile plaque formation in an Alzheimer disease model. *Microcirculation* **10,** 463–470
24. Donahue, J. E., Flaherty, S. L., Johanson, C. E., Duncan, J. A., 3rd, Silverberg, G. D., Miller, M. C., Tavares, R., Yang, W., Wu, Q., Sabo, E., Hovanesian, V., and Stopa, E. G. (2006) RAGE, LRP-1, and amyloid-β protein in Alzheimer's disease. *Acta Neuropathol.* **112,** 405–415
25. DeMattos, R. B., Bales, K. R., Cummins, D. J., Dodart, J. C., Paul, S. M., and Holtzman, D. M. (2001) Peripheral anti-A β antibody alters CNS and plasma A β clearance and decreases brain A β burden in a mouse model of Alzheimer's disease. *Proc. Natl. Acad. Sci. U.S.A.* **98,** 8850–8855
26. Herrmann, N., Chau, S. A., Kircanski, I., and Lanctôt, K. L. (2011) Current and emerging drug treatment options for Alzheimer's disease. A systematic review. *Drugs* **71,** 2031–2065
27. Pfeifer, M., Boncristiano, S., Bondolfi, L., Stalder, A., Deller, T., Staufenbiel, M., Mathews, P. M., and Jucker, M. (2002) Cerebral hemorrhage after

passive anti-Aβ immunotherapy. *Science* **298,** 1379
28. Wilcock, D. M., Morgan, D., Gordon, M. N., Taylor, T. L., Ridnour, L. A., Wink, D. A., and Colton, C. A. (2011) Activation of matrix metalloproteinases following anti-Aβ immunotherapy. Implications for microhemorrhage occurrence. *J. Neuroinflammation* **8,** 115
29. Kou, J., Kim, H., Pattanayak, A., Song, M., Lim, J. E., Taguchi, H., Paul, S., Cirrito, J. R., Ponnazhagan, S., and Fukuchi, K. (2011) Anti-amyloid-β single-chain antibody brain delivery via AAV reduces amyloid load but may increase cerebral hemorrhages in an Alzheimer's disease mouse model. *J. Alzheimers Dis.* **27,** 23–38
30. Selkoe, D. J. (2012) Preventing Alzheimer's disease. *Science* **337,** 1488–1492
31. Klaver, A. C., Finke, J. M., Digambaranath, J., Balasubramaniam, M., and Loeffler, D. A. (2010) Antibody concentrations to Aβ1–42 monomer and soluble oligomers in untreated and antibody-antigen-dissociated intravenous immunoglobulin preparations. *Int. Immunopharmacol.* **10,** 115–119
32. Dodel, R., Neff, F., Noelker, C., Pul, R., Du, Y., Bacher, M., and Oertel, W. (2010) Intravenous immunoglobulins as a treatment for Alzheimer's disease. Rationale and current evidence. *Drugs* **70,** 513–528
33. Blacklow, S. C., and Kim, P. S. (1996) Protein folding and calcium binding defects arising from familial hypercholesterolemia mutations of the LDL receptor. *Nat. Struct. Biol.* **3,** 758–762
34. Atkins, A. R., Brereton, I. M., Kroon, P. A., Lee, H. T., and Smith, R. (1998) Calcium is essential for the structural integrity of the cysteine-rich, ligand-binding repeat of the low-density lipoprotein receptor. *Biochemistry* **37,** 1662–1670
35. Meijer, A. B., Rohlena, J., van der Zwaan, C., van Zonneveld, A. J., Boertjes, R. C., Lenting, P. J., and Mertens, K. (2007) Functional duplication of ligand-binding domains within low-density lipoprotein receptor-related protein for interaction with receptor associated protein, α2-macroglobulin, factor IXa and factor VIII. *Biochim. Biophys. Acta* **1774,** 714–722
36. Obermoeller, L. M., Warshawsky, I., Wardell, M. R., and Bu, G. (1997) Differential functions of triplicated repeats suggest two independent roles for the receptor-associated protein as a molecular chaperone. *J. Biol. Chem.* **272,** 10761–10768
37. Croy, J. E., Shin, W. D., Knauer, M. F., Knauer, D. J., and Komives, E. A. (2003) All three LDL receptor homology regions of the LDL receptor-related protein bind multiple ligands. *Biochemistry* **42,** 13049–13057
38. Neels, J. G., van Den Berg, B. M., Lookene, A., Olivecrona, G., Pannekoek, H., and van Zonneveld, A. J. (1999) The second and fourth cluster of class A cysteine-rich repeats of the low density lipoprotein receptor-related protein share ligand-binding properties. *J. Biol. Chem.* **274,** 31305–31311
39. Herz, J., Goldstein, J. L., Strickland, D. K., Ho, Y. K., and Brown, M. S. (1991) 39-kDa protein modulates binding of ligands to low density lipoprotein receptor-related protein/α2-macroglobulin receptor. *J. Biol. Chem.* **266,** 21232–21238
40. Deane, R., Bell, R. D., Sagare, A., and Zlokovic, B. V. (2009) Clearance of amyloid-β peptide across the blood-brain barrier. Implication for therapies in Alzheimer's disease. *CNS Neurol. Disord. Drug Targets* **8,** 16–30
41. Kayed, R., Head, E., Thompson, J. L., McIntire, T. M., Milton, S. C., Cotman, C. W., and Glabe, C. G. (2003) Common structure of soluble amyloid oligomers implies common mechanism of pathogenesis. *Science* **300,** 486–489
42. Kayed, R., Head, E., Sarsoza, F., Saing, T., Cotman, C. W., Necula, M., Margol, L., Wu, J., Breydo, L., Thompson, J. L., Rasool, S., Gurlo, T., Butler, P., and Glabe, C. G. (2007) Fibril specific, conformation dependent antibodies recognize a generic epitope common to amyloid fibrils and fibrillar oligomers that is absent in prefibrillar oligomers. *Mol. Neurodegener.* **2,** 18
43. Mackic, J. B., Weiss, M. H., Miao, W., Kirkman, E., Ghiso, J., Calero, M., Bading, J., Frangione, B., and Zlokovic, B. V. (1998) Cerebrovascular accumulation and increased blood-brain barrier permeability to circulating Alzheimer's amyloid β peptide in aged squirrel monkey with cerebral amyloid angiopathy. *J. Neurochem.* **70,** 210–215
44. Deane, R., Sagare, A., Hamm, K., Parisi, M., LaRue, B., Guo, H., Wu, Z., Holtzman, D. M., and Zlokovic, B. V. (2005) IgG-assisted age-dependent clearance of Alzheimer's amyloid β peptide by the blood-brain barrier neonatal Fc receptor. *J. Neurosci.* **25,** 11495–11503
45. Wahrle, S. E., Jiang, H., Parsadanian, M., Legleiter, J., Han, X., Fryer, J. D., Kowalewski, T., and Holtzman, D. M. (2004) ABCA1 is required for normal central nervous system ApoE levels and for lipidation of astrocyte-secreted apoE. *J. Biol. Chem.* **279,** 40987–40993
46. Deacon, R. M. (2009) Burrowing. A sensitive behavioural assay, tested in five species of laboratory rodents. *Behav. Brain Res.* **200,** 128–133
47. Deane, R., Singh, I., Sagare, A. P., Bell, R. D., Ross, N. T., LaRue, B., Love, R., Perry, S., Paquette, N., Deane, R. J., Thiyagarajan, M., Zarcone, T., Fritz, G., Friedman, A. E., Miller, B. L., and Zlokovic, B. V. (2012) A multimodal RAGE-specific inhibitor reduces amyloid β-mediated brain disorder in a mouse model of Alzheimer disease. *J. Clin. Invest.* **122,** 1377–1392
48. Zhong, Z., Deane, R., Ali, Z., Parisi, M., Shapovalov, Y., O'Banion, M. K., Stojanovic, K., Sagare, A., Boillee, S., Cleveland, D. W., and Zlokovic, B. V. (2008) ALS-causing SOD1 mutants generate vascular changes prior to motor neuron degeneration. *Nat. Neurosci.* **11,** 420–422
49. Horn, I. R., van den Berg, B. M., van der Meijden, P. Z., Pannekoek, H., and van Zonneveld, A. J. (1997) Molecular analysis of ligand binding to the second cluster of complement-type repeats of the low density lipoprotein receptor-related protein. Evidence for an allosteric component in receptor-associated protein-mediated inhibition of ligand binding. *J. Biol. Chem.* **272,** 13608–13613
50. Westein, E., Denis, C. V., Bouma, B. N., and Lenting, P. J. (2002) The α-chains of C4b-binding protein mediate complex formation with low density lipoprotein receptor-related protein. *J. Biol. Chem.* **277,** 2511–2516
51. Leyte, A., Mertens, K., Distel, B., Evers, R. F., De Keyzer-Nellen, M. J., Groenen-Van Dooren, M. M., De Bruin, J., Pannekoek, H., Van Mourik, J. A., and Verbeet, M. P. (1989) Inhibition of human coagulation factor VIII by monoclonal antibodies. *Biochem. J.* **263,** 187–194
52. Mackic, J. B., Bading, J., Ghiso, J., Walker, L., Wisniewski, T., Frangione, B., and Zlokovic, B. V. (2002) Circulating amyloid-β peptide crosses the blood-brain barrier in aged monkeys and contributes to Alzheimer's disease lesions. *Vascul. Pharmacol.* **38,** 303–313
53. Dodel, R., Hampel, H., Depboylu, C., Lin, S., Gao, F., Schock, S., Jäckel, S., Wei, X., Buerger, K., Höft, C., Hemmer, B., Möller, H. J., Farlow, M., Oertel, W. H., Sommer, N., and Du, Y. (2002) Human antibodies against amyloid β peptide. A potential treatment for Alzheimer's disease. *Ann. Neurol.* **52,** 253–256
54. Szabo, P., Mujalli, D. M., Rotondi, M. L., Sharma, R., Weber, A., Schwarz, H. P., Weksler, M. E., and Relkin, N. (2010) Measurement of anti-β amyloid antibodies in human blood. *J. Neuroimmunol.* **227,** 167–174
55. Balakrishnan, K., Andrei-Selmer, L. C., Selmer, T., Bacher, M., and Dodel, R. (2010) Comparison of intravenous immunoglobulins for naturally occurring autoantibodies against amyloid-β. *J. Alzheimers Dis.* **20,** 135–143
56. Bach, J. P., and Dodel, R. (2012) Naturally occurring autoantibodies against β-amyloid. *Adv. Exp. Med. Biol.* **750,** 91–99
57. Du, Y., Dodel, R., Hampel, H., Buerger, K., Lin, S., Eastwood, B., Bales, K., Gao, F., Moeller, H. J., Oertel, W., Farlow, M., and Paul, S. (2001) Reduced levels of amyloid β-peptide antibody in Alzheimer disease. *Neurology* **57,** 801–805
58. Britschgi, M., Olin, C. E., Johns, H. T., Takeda-Uchimura, Y., LeMieux, M. C., Rufibach, K., Rajadas, J., Zhang, H., Tomooka, B., Robinson, W. H., Clark, C. M., Fagan, A. M., Galasko, D. R., Holtzman, D. M., Jutel, M., Kaye, J. A., Lemere, C. A., Leszek, J., Li, G., Peskind, E. R., Quinn, J. F., Yesavage, J. A., Ghiso, J. A., and Wyss-Coray, T. (2009) Neuroprotective natural antibodies to assemblies of amyloidogenic peptides decrease with normal aging and advancing Alzheimer's disease. *Proc. Natl. Acad. Sci. U.S.A.* **106,** 12145–12150
59. DeMattos, R. B., Bales, K. R., Cummins, D. J., Paul, S. M., and Holtzman, D. M. (2002) Brain to plasma amyloid-β efflux. A measure of brain amyloid burden in a mouse model of Alzheimer's disease. *Science* **295,** 2264–2267
60. Relkin, N. R., Szabo, P., Adamiak, B., Burgut, T., Monthe, C., Lent, R. W., Younkin, S., Younkin, L., Schiff, R., and Weksler, M. E. (2009) 18-Month study of intravenous immunoglobulin for treatment of mild Alzheimer disease. *Neurobiol. Aging* **30,** 1728–1736
61. Shayan, G., Adamiak, B., Relkin, N. R., and Lee, K. H. (2012) Longitudinal analysis of novel Alzheimer's disease proteomic cerebrospinal fluid biomarkers during intravenous immunoglobulin therapy. *Electrophoresis* **33,**

1975–1979
62. Matsuoka, Y., Saito, M., LaFrancois, J., Saito, M., Gaynor, K., Olm, V., Wang, L., Casey, E., Lu, Y., Shiratori, C., Lemere, C., and Duff, K. (2003) Novel therapeutic approach for the treatment of Alzheimer's disease by peripheral administration of agents with an affinity to β-amyloid. *J. Neurosci.* **23,** 29–33
63. Hirko, A. C., Meyer, E. M., King, M. A., and Hughes, J. A. (2007) Peripheral transgene expression of plasma gelsolin reduces amyloid in transgenic mouse models of Alzheimer's disease. *Mol. Ther.* **15,** 1623–1629
64. Wu, Z., Guo, H., Chow, N., Sallstrom, J., Bell, R. D., Deane, R., Brooks, A. I., Kanagala, S., Rubio, A., Sagare, A., Liu, D., Li, F., Armstrong, D., Gasiewicz, T., Zidovetzki, R., Song, X., Hofman, F., and Zlokovic, B. V. (2005) Role of the MEOX2 homeobox gene in neurovascular dysfunction in Alzheimer disease. *Nat. Med.* **11,** 959–965
65. Tamaki, C., Ohtsuki, S., Iwatsubo, T., Hashimoto, T., Yamada, K., Yabuki, C., and Terasaki, T. (2006) Major involvement of low-density lipoprotein receptor-related protein 1 in the clearance of plasma free amyloid β-peptide by the liver. *Pharm. Res.* **23,** 1407–1416
66. Zloković, B. V., Lipovac, M. N., Begley, D. J., Davson, H., and Rakić, L. (1987) Transport of leucine-enkephalin across the blood-brain barrier in the perfused guinea pig brain. *J. Neurochem.* **49,** 310–315
67. Andersen, O. M., Christensen, P. A., Christensen, L. L., Jacobsen, C., Moestrup, S. K., Etzerodt, M., and Thogersen, H. C. (2000) Specific binding of α-macroglobulin to complement-type repeat CR4 of the low-density lipoprotein receptor-related protein. *Biochemistry* **39,** 10627–10633
68. Andersen, O. M., Reiche, J., Schmidt, V., Gotthardt, M., Spoelgen, R., Behlke, J., von Arnim, C. A., Breiderhoff, T., Jansen, P., Wu, X., Bales, K. R., Cappai, R., Masters, C. L., Gliemann, J., Mufson, E. J., Hyman, B. T., Paul, S. M., Nykjaer, A., and Willnow, T. E. (2005) Neuronal sorting protein-related receptor sorLA/LR11 regulates processing of the amyloid precursor protein. *Proc. Natl. Acad. Sci. U.S.A.* **102,** 13461–13466
69. Gregory, J. L., Prada, C. M., Fine, S. J., Garcia-Alloza, M., Betensky, R. A., Arbel-Ornath, M., Greenberg, S. M., Bacskai, B. J., and Frosch, M. P. (2012) Reducing available soluble β-amyloid prevents progression of cerebral amyloid angiopathy in transgenic mice. *J. Neuropathol. Exp. Neurol.* **71,** 1009–1017
70. Huang, Y., and Mucke, L. (2012) Alzheimer mechanisms and therapeutic strategies. *Cell* **148,** 1204–1222
71. Galluzzi, S., Geroldi, C., Amicucci, G., Bocchio-Chiavetto, L., Bonetti, M., Bonvicini, C., Cotelli, M., Ghidoni, R., Paghera, B., Zanetti, O., and Frisoni, G. B. (2013) Supporting evidence for using biomarkers in the diagnosis of MCI due to AD. *J. Neurol.* **260,** 640–650